Deep Labrador Current and its variability in 1996–2005

Marcus Dengler,[1] Jürgen Fischer,[1] Friedrich A. Schott[1] and Rainer Zantopp[1]

Received 25 April 2006; revised 31 August 2006; accepted 13 September 2006; published 17 October 2006.

[1] Long term mooring observations show a substantial warming of the Deep Labrador Current (DLC) during the last decade. In this paper we address the question of whether these water mass changes are accompanied by comparable changes in the deep western boundary current. Individual estimates of alongshore current from moored instruments and transports from Lowered ADCP sections indicate a systematic increase of the boundary current strength on the order of 15% of the mean from the period prior to 1999 to the period thereafter. A combination of these measurements allows the indexing of DLC intensity over the last decade.
Citation: Dengler, M., J. Fischer, F. A. Schott, and R. Zantopp (2006), Deep Labrador Current and its variability in 1996–2005, *Geophys. Res. Lett.*, *33*, L21S06, doi:10.1029/2006GL026702.

1. Introduction

[2] Within the subpolar North Atlantic a vigorous deep western boundary current (DWBC) carries ventilated North Atlantic Deep Water (NADW) from the overflow regions and from the Labrador Sea southward. Labrador Sea Water (LSW), the shallowest component of the NADW, is formed by deep convection in the Labrador Sea. Below the LSW, water masses are encountered that enter the western subpolar North Atlantic via the Gibbs Fracture Zone, the Gibbs Fracture Zone Water (GFZW), and through Denmark Strait, the Denmark Strait Overflow Water (DSOW).

[3] Significant thermohaline variability is observed in all three deep water masses [*Lazier et al.*, 2002; *Stramma et al.*, 2004]. Particularly dramatic changes occurred in the LSW throughout the most recent decade: from cold and fresh at the end of the intense convection period in the early 90's to more saline and warmer in the period thereafter [*Lazier et al.*, 2002]. It is this thermohaline variability that can be traced to the subtropical and tropical Atlantic by potential vorticity anomalies [*Talley and McCartney*, 1982] and chemical tracers [*Fine and Molinari*, 1988], the latter of which may be taken as a proxy for the input of anthropogenic CO_2 and its subsequent spreading.

[4] Less is known about the strength and variability of the circulation in the deep subpolar gyre. Individual estimates of the flow along the Labrador shelf break show transports much larger than required for the thermohaline circulation [*Pickart et al.*, 2002; *Fischer et al.*, 2004, hereinafter referred to as FSD04]. A series of complex recirculation cells adjacent to the cyclonic boundary current, unknown until recently [*Lavender et al.*, 2000; *Fischer and Schott*, 2002], complicate the exchange of interior water masses with the boundary current. Model studies [e.g., *Eden and Willebrand*, 2001] showed a delayed response (2–3 years) of the thermohaline circulation to anomalous forcing and convection in the Labrador Sea. Recently, such variability has been diagnosed from altimeter data by *Häkkinen and Rhines* [2004, hereinafter referred to as HR04]. In their analysis, a decline of the shallow subpolar circulation throughout the 1990s was postulated by an EOF analysis of sea surface heights. Current meter records from the DWBC in the Labrador Sea deployed between 1996 and 1998, the period analyzed by HR04, support the weakening circulation trend and suggest that the late 1990s decline extends deep into the water column. Their analysis suggested that the weakening of the DWBC was linked to a corresponding weakening trend of the net heat fluxes in the subpolar North Atlantic.

[5] Here, we use current meter and temperature records from the Deep Labrador Current (DLC) at 1500 m depth to describe its interannual variability during the period from 1996 to 2005. Repeated shipboard velocity sections are used to analyze the DLC structure and its variability at two locations, 53°N and 56°N. Finally, an index for the boundary current strength is presented which is used as an indicator for the variability of Labrador Sea Water transport.

2. Data and Methods

2.1. Moorings

[6] Since 1997 a moored array was deployed near the exit of the Labrador Sea along 53°N (Figure 1). For the first two years this array consisted of 5 moorings covering the flow near the shelf break out to the deep Labrador Sea (FSD04). During the period 1999 to 2003 the array was reduced to three moorings of which we unfortunately lost the central mooring during the first two years. For the last two years (2003 to 2005) only the central mooring (K9, at 2800 m water depth) was continued. Farther up north, at Hamilton Bank, a boundary current mooring (K2, see Figure 1) was deployed since summer 1996. This mooring was located at about the same water depth as K9 at 53°N, with some shifts in location during different deployment periods (water depth was 2400 m in the first two years, and 2800 m thereafter).

[7] In terms of instrument coverage, the focus of the observational program was on the LSW layer, and thus the 1500 m level was well instrumented. Here, this subset of available current meter records is analyzed. All current time series are detided by application of a 40h low pass filter and subsequently subsampled to 12h resolution.

2.2. Velocity Sections

[8] Two sections running perpendicular to the shelf break in the Labrador Sea were repeatedly occupied during seven cruises: in August 1996, July of 1997, 1998 and 1999, June 2001, September 2003, and August 2005. One section ran along the mooring line at 53°N, the other one along the western part of WOCE line AR7W at about 56°N (Figure 1).

[1]Leibniz-Institut für Meereswissenschaften an der Universität Kiel, (IFM-GEOMAR), Kiel, Germany.

0094-8276/06/2006GL026702

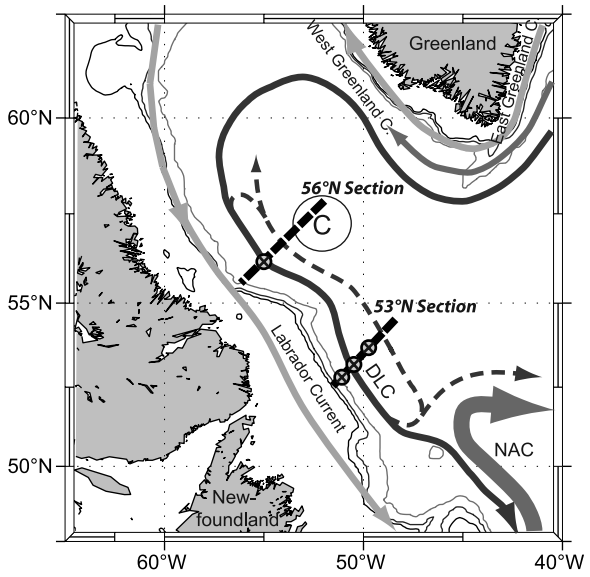

Figure 1. Schematic circulation diagram of the Labrador Sea. Location of the repeated sections are indicated by thick dashed lines and mooring positions by crossed circles.

Station data included conductivity-temperature-depth (CTD) data and direct velocity profiles collected with lowered acoustic Doppler current profilers (LADCP). A subset of five LADCP sections has been presented by FSD04 but is reanalyzed here using a new processing algorithm. All LADCP data were post-processed using an inverse technique [*Visbeck*, 2002] that constrains the resulting velocity profiles to on-station shipboard ADCP data and bottom track velocities. Furthermore, barotropic tidal currents were eliminated by using a global tidal model [*LeProvost et al.*, 1994].

[9] Due to energetic high frequency variability (FSD04) at small spatial scales [e.g., *Lilly et al.*, 2003] within the Labrador Sea boundary current regime not fully resolved by station spacing, we refrain from estimating transports from individual velocity sections. Instead, we present averaged velocity sections using all available LADCP profiles collected during distinct time periods. Section means are derived by interpolating the alongshore velocity component onto a 10 km by 10 m grid using Gaussian weights. Transports are then determined for different layers separated by isopycnal surfaces which in turn are determined from the summer CTD data.

[10] The standard deviation of velocity at both sections, determined from ensembles of six to 10 adjacent current profiles, is between 0.05 m s^{-1} and 0.08 m s^{-1} throughout the water column and slightly higher than the measurement error (0.04 m s^{-1}). We use a Monte Carlo technique to estimate transport uncertainties: Random velocity uncertainties of Gaussian distribution scaled to the standard deviation of adjacent ensembles are added to the individual velocity profiles in 100 different realizations, and standard deviations of the resulting layer transports are calculated. These standard deviations are used as a proxy for transport uncertainty.

3. Current and Temperature Variability

[11] Within the density range of upper and classical LSW, dramatic temperature changes are observed throughout the deployment period. In the central Labrador Sea, convection has generally weakened since 1994, and the 1500 m depth level has not been ventilated since winter of 1996/97 [*Lazier et al.*, 2002]. Within the DLC, we observe an almost linear increase of temperature (Figure 2a, see also Figure 3 for position with respect to the DLC) at 1500 m depth at 53°N and 56°N. From 1997 to 2003, temperature rises from 2.9°C to 3.25°C at a rate of 0.05°C per year. After 2003, the warming appears to have ceased as indicated by the flattening of the temperature time series. Farther along the route of the DWBC, at the tail of the Grand Banks, a similar temperature increase of 0.05°C $year^{-1}$ is observed [*Schott et al.*, 2006].

[12] During the deployment period reported here, the warming of the DLC is not accompanied by a weakening trend in alongshore flow within the LSW layer of the DLC (Figure 2b). Instead, the current meter time series from 1500 m depth exhibit intraseasonal to interannual variability of the boundary current velocity at both locations. However, the near continuous records from K2 (56°N) and K9 (53°N) show increasing southward alongshore velocities after 1999 when compared to the alongshore currents between 1997 and 1999. For K9, the average alongshore velocity computed over the time span from 1997 to 1999 yields 0.12 m s^{-1}, while the average from 2001 to 2005 yields 0.15 m s^{-1}. It should be noted that K2 was deployed at two different positions with respect to the core of the DLC and the time series are not directly comparable. However, as will be explained below, the mooring relocation into deeper waters in June 1998 should have led to slightly lower southward velocities. In contrast, average alongshore velocities here increase from 0.14 m s^{-1} in 1996 to 1999 to 0.17 m s^{-1} between 2001 and 2003. Annual average across-shore flow in all time series is smaller than 0.01 m s^{-1} and lacks significance.

4. DLC Structure and Transports

[13] DLC structure and transports are discussed for depth layers separated by average isopycnal boundaries calculated from all available CTD data. We choose the depth interval between isopycnals 27.68 and 27.80 to reflect the upper and classical LSW layer. The depth distribution of these two

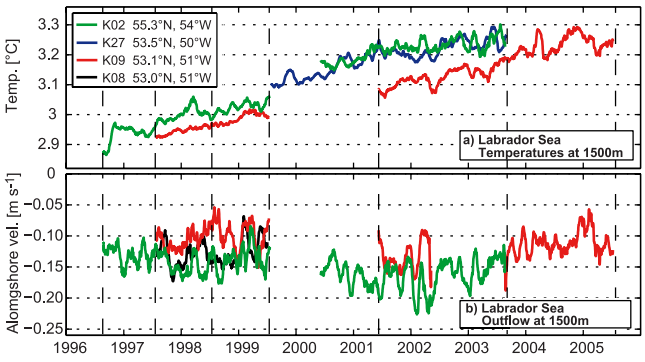

Figure 2. (top) Evolution of potential temperature and (bottom) alongshore velocity at 1500 m depth in the boundary current at 53°N (moorings K8, K9, K27) and at 56°N (mooring K2). Vertical dashed lines indicate cruise periods.

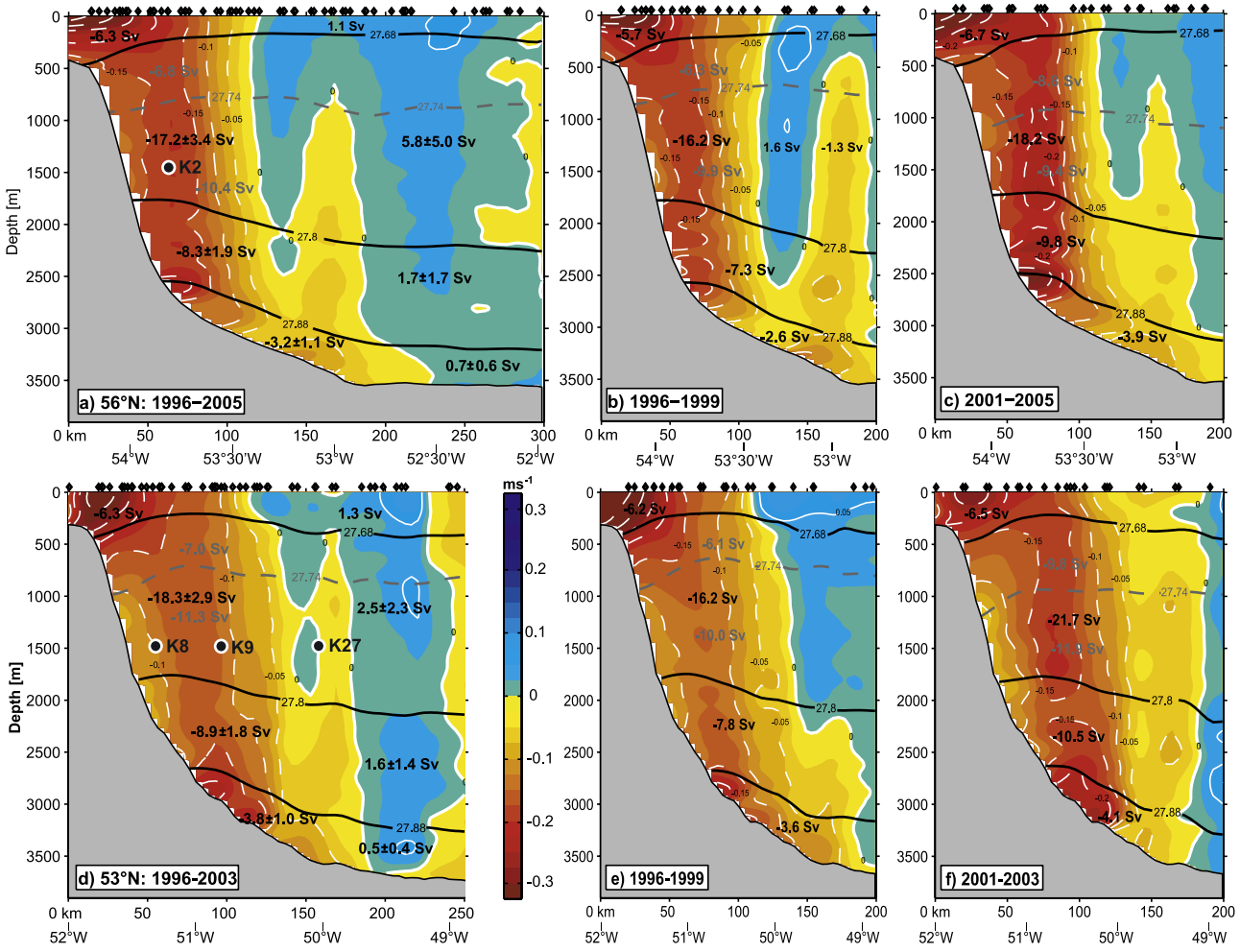

Figure 3. (a–c) Average alongshore LADCP velocities from the 56°N and (d–f) 53°N sections for different time intervals: from 1996 to 2005 (2003) in Figures 3a and 3d, from 1996–1999 in Figures 3b and 3e, and from 2001 to 2005 (2003) in Figures 3c and 3f. Contour interval is 0.025 m s^{-1}. Positive values indicate northwestward flow. Bold numbers represent transports in Sverdrup between isopycnal boundaries. Diamonds indicated position of profiles used in average, thick black circles show positions of moored time series.

isopycnals has varied the least, while the interface isopycnal 27.74 has gradually deepened throughout the observational period. Two deeper water masses, GFZW and DSOW, are distinguished by the isopycnal boundaries $27.80 \leq \sigma_\theta \leq 27.88$ for the former, and $\sigma_\theta > 27.88$ for the latter. It should be noted, however, that the depth distribution of the isopycnal boundaries varies on seasonal and interannual time scales and thus introduces transport variability not resolved in our estimates.

[14] The mean alongshore flow at 56°N (Figure 3a) was calculated from 82 LADCP profiles collected during seven repeat sections between 1996 and 2005. The DLC extends about 120 km offshore and shows a pronounced barotropic component. Above 2000 m depth, its core is detached from the continental slope. Velocities in the DLC core are 0.16 to 0.18 m s^{-1} within the LSW and GFZW layer. The position of a velocity maximum in the DSOW layer varies among individual occupations, but it is always found onshore of 52°45′W. Immediately offshore of the DLC, weak northwestward flow is found in 6 of the 7 individual ship sections. The average northwestward flow determined from 17 profiles is between 0.02 and 0.03 m s^{-1}. Estimates of the uncertainties show that the recirculation is small but significant.

[15] The mean alongshore flow at 53°N was determined from 65 profiles collected during six cruises from 1996 to 2003. During the September 2005 survey, a vigorous eddy was located in the DLC, leading to very high southwestward velocities (>0.35 m s^{-1}). As the moored velocity records indicated that these DLC velocities were observed during less than 4% of the total deployment period only, we omitted this section in the average section. At 53°N, the DLC extends from the shelf break to about 150 km offshore (Figure 3d). It exhibits a similar structure as observed along 56°N. At 53°N however, the boundary current is somewhat wider and has slightly lower core velocities, most likely due to less steep topography at this location. In the LSW and GFZW layer, average core velocities are 0.13 m s^{-1} to 0.15 m s^{-1}. The DSOW core is more focused compared to the upstream section while average core velocities (0.19 m s^{-1} to 0.22 m s^{-1}) are higher. The return flow is narrower and has a width of only about 70 km. Average

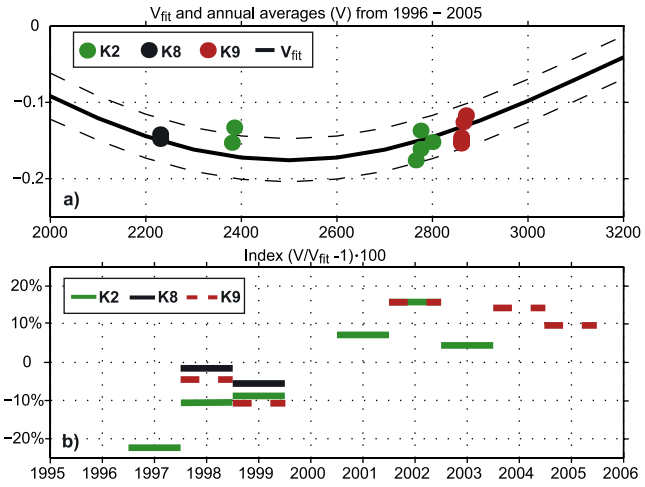

Figure 4. (top) Excerpt of cross stream function (V_{fit}) vs. bottom topography from FSD04 including 95% confidence intervals (dashed lines). Filled circles represent annual mean alongshore velocities from the 1500 m time series. (bottom) Annual means of LSW transport index ($V/V_{fit} - 1$) defined as the anomaly of the ratio of individual annual alongshore means (V) to the DCL structure function (V_{fit}) at its corresponding water depth.

northwestward speed in the recirculation of 0.02 m s^{-1} to 0.04 m s^{-1} is marginally significant as the uncertainty is slightly below 0.02 m s^{-1}. Compared to a 5-section subset previously given by FSD04, the use of reprocessed LADCP data plus the profiles from the additional section has reduced uncertainties in the DLC structure and the recirculation. Improvements are most noticeable in the near bottom circulation where the use of bottom track in the inverse method has lowered the errors in the velocity profiles.

[16] At 56°N, the total DLC transport is 28.7 ± 6.4 Sv. More than half of the transport (17.2 ± 3.4Sv) is accomplished within the LSW layer, while the GFZW layer and DSOW carry 8.3 ± 1.9 Sv and 3.2 ± 1.0 Sv, respectively. Within the recirculation, 8.2 ± 7.2 Sv of deep water are recirculating northeastward. The DLC transport at 53°N of 31.0 ± 4.7 Sv is slightly higher than at 56°N, but within the uncertainties, and so are the transports for individual layers. When including the September 2005 section, the average DLC transport increases to 34.6 Sv. Transports within the recirculation, however, are only 4.6 ± 4.1 Sv, about half of transport at 56°N. It is thus likely that a substantial part of the recirculation at 56°N is supplied either from the DLC north of the 53°N, perhaps at Hamilton Bank or is part of an anticyclonic circulation in the interior of the Labrador Sea.

[17] To compare the structure of the DLC during the weaker and stronger 1500m alongshore flow periods diagnosed from the current records, we also computed the average boundary current structure from the data of four cruises between 1996 to 1999 (Figures 3b and 3e) and from three cruises after 2000 (Figures 3c and 3f) separately. At 56°N as well as 53°N, a considerably weaker DLC is found during the first period compared to the period after 2000. The velocity increase within the LSW layer varies between 0.02 m s^{-1} and 0.05 m s^{-1} during the later period. Furthermore, the strengthening of the DLC is not limited to the upper layers but seems to extend throughout the water column. In fact, the data suggest that the strengthening of the DLC during the later period is a near barotropic response as the increase of velocity is of similar magnitude throughout the whole water column. It should be noted that the uncertainty of alongshore velocity in the sections averaged over the two time periods is on the order of 0.02 m s^{-1} to 0.04 m s^{-1}. Thus, the DLC strengthening is marginally significant. However, the deeper mooring records (2800 m) from K2 and K9 (not shown) also show increased southward alongshore velocities after 2000 and support the findings above.

[18] Transports in the different water mass layers also seem to have increased in the latter period. At 56°N the total DLC transport increases by 5.8 Sv while an increase of 8.7 Sv is suggested at 53°N. However, considering the uncertainty of our estimates, these differences lack statistical confidence.

5. Boundary Current Index

[19] The current meter data (FSD04) strongly suggest that records from near the center of the DLC are good indicators for the strength of the current and its transport, at least for the LSW layer. This is illustrated by the location of the moored records in Figures 3a and 3d and has been tested quantitatively by correlating individual records of mooring K9 from the first deployment of the 53°N array with the two year long records of the respective transport from the array given by FSD04. Correlation coefficients (r) are 0.66 for the transport within the LSW layer (i.e., the transport between about 800 m and 2000 m depth) and 0.50 for the total deep water transport at 10-day resolution. Both are significant at the 95% level. Correlations for time scales longer than 60-days are 0.80 for the LSW transports and 0.56 for the total transport. This illustrates that the 1500 m records from approximately the center of the boundary current can be interpreted as an index for the LSW transport along the western boundary and, with somewhat less confidence, for the total DLC strength.

[20] Due to slightly different locations of some moorings during subsequent redeployment periods, we use a reference cross-stream structure of the boundary current to compare individual annual mean velocities. Such a cross-stream structure of the DLC along the continental slope has been established by FSD04 on the basis of Lagrangian trajectories and current meter records at the 1500 m depth level. As the DLC follows potential vorticity (f/H) contours, the cross-stream flow structure is best defined by bottom topography. The best fit of bottom topography to the Lagrangian and Eulerian velocity data using a polynomial curve and its 95% confidence interval for the 2000 m to 3000 m bottom topography range is shown in Figure 4a. Annual mean alongshore velocities for the different current meter record at their corresponding water depth are also displayed. Most of the annual mean currents are within the 95% confidence interval, i.e. within a band of ±0.025 m s^{-1} around the mean DLC curve.

[21] We define the LSW index ($V/V_{fit} - 1$) as the anomaly of the ratio of the individual annual alongshore means (V) to the DCL structure function (V_{fit}) at its corresponding water depth. The temporal evolution of the index (Figure 4b) shows weak but systematic variability,

and there is reasonable agreement between the index values at 53°N and at 56°N. Low values (−10% to 0%) are found during the period from 1996 to 1999, while from 2001 onward, the index increases to above its mean (5–15%) and remains at its high level until the termination of the record in summer 2005.

[22] The uncertainty of the LSW transport index can be estimated from the standard deviation of the annual mean currents which is in the range of 0.05–0.1 m s^{-1} and is mainly due to high frequency variability with time scales of less than 20 days. Thus the standard error of the annual mean is conservatively estimated at 0.015 m s^{-1}, and translates into an index uncertainty of about 10%. This uncertainty also corresponds well to the variability of the index for records from different locations from the same year.

6. Discussion

[23] We present moored records from two locations in the DLC and averaged ship sections from 53°N and 56°N that indicate an increased southward alongshore flow of 10 to 20% from the late 1990s to the years after 1999. The significance of each individual estimate is marginal, but their agreement in magnitude and phase of the onset of the DLC strengthening substantiates the results.

[24] A strengthening of the DLC despite the lack of deep convection and continuing low net heat fluxes in the Labrador Sea throughout the observational period requires an additional forcing mechanism controlling the DLC. In a recent sequence of OGCM simulations using interannually-varying heat fluxes and wind stress, *Böning et al.* [2006] showed that decadal variability of the western boundary current in the Labrador Sea is driven by changes in both, heat flux and wind stress variability. While the model hindcasts successfully reproduce the decline of sea surface height during the 1990s, as noted by HR04, and an associated weakening of the boundary current in the Labrador Sea of 7 to 8 Sv, they also show a boundary current strengthening from 1999 to 2003 of 4 to 5 Sv. This strengthening was not present in hindcast simulations, which permitted interannual heat flux variations but restricted wind stress forcing to a climatological annual cycle.

[25] The question of how the observed temporal evolution of LSW transport relates to total NADW transport variability remains an issue for future research, and more effort is required to prove its relevance for monitoring the MOC variability as suggested by modeling results of *Böning et al.* [2006].

[26] **Acknowledgments.** This study was supported by the Deutsche Forschungsgemeinschaft in the framework of Sonderforschungsbereich 460 *Dynamik thermohaliner Zirkulationsschwankungen*.

References

Böning, C., M. Scheinert, J. Dengg, A. Biastoch, and A. Funk (2006), Decadal variability of subpolar gyre transport and its reverberation in the North Atlantic overturning, *Geophys. Res. Lett.*, *33*, L21S01, doi:10.1029/2006GL026906.

Eden, C., and J. Willebrand (2001), Mechanism of interannual to decadal variability of the North Atlantic circulation, *J. Clim.*, *14*, 2266–2280.

Fine, R. A., and R. L. Molinari (1988), A continuous deep western boundary current between Abaco (26.5°N) and Barbados (13°N), *Deep Sea Res., Part A*, *35*, 1441–1450.

Fischer, J., and F. Schott (2002), Labrador Sea Water tracked by profiling floats—From the boundary current into the open North Atlantic, *J. Phys. Oceanogr.*, *32*, 573–584.

Fischer, J., F. Schott, and M. Dengler (2004), Boundary circulation at the exit of the Labrador Sea, *J. Phys. Oceanogr.*, *34*, 1548–1570.

Häkkinen, S., and P. B. Rhines (2004), Decline of subpolar North Atlantic circulation during the 1990s, *Science*, *304*, 555–559.

Lavender, K. L., R. E. Davis, and W. B. Owens (2000), Mid-depth recirculation observed in the interior Labrador and Irminger seas by direct velocity measurements, *Nature*, *407*, 66–69.

Lazier, J. R. N., R. Hendry, A. Clarke, I. Yashayaev, and P. Rhines (2002), Convection and restratification in the Labrador Sea, 1990–2000, *Deep Sea Res., Part I*, *49*, 1819–1835.

LeProvost, C., M. L. Genco, and F. Lyard (1994), Spectroscopy of the world ocean tides from a finite element hydrodynamic model, *J. Geophys. Res.*, *99*, 24,777–24,797.

Lilly, J. M., P. B. Rhines, F. A. Schott, K. Lavender, J. Lazier, U. Send, and E. d'Asaro (2003), Observations of the Labrador Sea eddy field, *Prog. Oceanogr.*, *59*, 75–176.

Pickart, R. S., D. J. Torres, and R. A. Clarke (2002), Hydrography of the Labrador Sea during active convection, *J. Phys. Oceanogr.*, *32*, 428–457.

Schott, F. A., J. Fischer, M. Dengler, and R. Zantopp (2006), Variability of the deep western boundary current east of the Grand Banks, *Geophys. Res. Lett.*, *33*, L21S07, doi:10.1029/2006GL026563.

Stramma, L., D. Kieke, M. Rhein, F. Schott, I. Yashayaev, and K. P. Koltermann (2004), Deep water changes at the western boundary of the subpolar North Atlantic during 1996 to 2001, *Deep Sea Res., Part I*, *51*, 1033–1056.

Talley, L. D., and M. S. McCartney (1982), Distribution and circulation of Labrador Sea Water, *J. Phys. Oceanogr.*, *12*, 1189–1205.

Visbeck, M. (2002), Deep velocity profiling using lowered acoustic Doppler current profilers: Bottom track and inverse solutions, *J. Atmos. Oceanic Technol.*, *19*, 794–807.

M. Dengler, J. Fischer, F. A. Schott, and R. Zantopp, IFM-GEOMAR, FB1/PO, Düsternbrooker Weg 20, D-24105 Kiel, Germany. (mdengler@ifm-geomar.de)